NANO LETTERS

2005
Vol. 5, No. 11
2310−2313

Nanoscale Optical Imaging of Excitons in Single-Walled Carbon Nanotubes

Achim Hartschuh,*,† Huihong Qian,† Alfred J. Meixner,† Neil Anderson,‡ and Lukas Novotny‡

Institute of Physical and Theoretical Chemistry, University of Tuebingen, Tuebingen, Germany, and The Institute of Optics, University of Rochester, Rochester, New York 14627

Received September 5, 2005

ABSTRACT

We present simultaneous near-field photoluminescence (PL) and Raman imaging of single-walled carbon nanotubes (SWNTs) with a spatial resolution better than 15 nm. Highly localized excitation is used to visualize the spatial extent of the contributing excited states. For SWNTs on glass, we typically observe highly confined PL from short segments of about 20 nm in length. The PL from micelle-encapsulated SWNTs on mica is extended along the tube up to several hundreds of nanometers. We find that near-field enhancement is much stronger for photoluminescence than for Raman scattering, an observation that is explained by the low intrinsic quantum yield of SWNTs.

Semiconducting single-walled carbon nanotubes (SWNTs) are photoluminescent quasi-one-dimensional quantum wires with great promise for application in photonics and opto- and nanoelectronics. A widespread utilization in optical devices, however, appears to be constrained by their low effective photoluminescence quantum yield which, being on the order of 10^{-3} to 10^{-4},[1,2] indicates that the excited state relaxation is dominated by very efficient nonradiative decay channels. Trapping of excitons at impurity sites or at structural defects as well as coupling or branching to optically inactive excitons are discussed as competing processes to radiative relaxation.[1,3−7] Single tube measurements, on the other hand, revealed both tube-to-tube variations of emission energies[8,9] and excited-state lifetimes[7] for micelle-encapsulated tubes indicating a significant role of defects and environmental perturbations. Similarly, these localized perturbations can be expected to limit the spatial extent of delocalized excitonic states along a tube and thus reduce the nanotube luminescence efficiency.

Recently, we demonstrated a technique for near-field imaging of SWNTs by detecting their Raman scattering signal with a spatial resolution of 10−20 nm and used it to investigate structural defects along individual tubes.[10,11] In this technique, enhanced optical fields close to a laser illuminated metal tip are used to locally excite the optical response of a sample. Tip-enhanced near-field microscopy has also been applied to excite locally the fluorescence of single molecules.[12,13] Here we show that this technique allows for simultaneous near-field Raman and photoluminescence (PL) imaging of SWNTs with a spatial resolution of better than 15 nm. This offers the unique possibility to compare the enhancement effect quantitatively and simultaneously for both signals. We find that near-field imaging of different samples, including frequently studied micelle-encapsulated SWNTs and SWNTs directly deposited on glass, exhibit a varying degree of localization of PL.

Our experimental setup is based on an inverted optical microscope with an *x,y* scan stage for raster scanning a transparent sample with SWNTs. A laser beam ($\lambda = 632.8$ nm, 60−800 μW) is reflected by a nonpolarizing beam splitter (50% transmission) and focused by a high numerical aperture objective (1.25 NA) on the sample surface. A sharp gold tip is positioned in the focus of the beam and maintained above the sample surface at a distance of 2 nm by means of a sensitive shear-force feedback mechanism.[14] PL emission and Raman scattered light is collected with the same objective, transmitted by the beam splitter, and filtered by a notch filter. PL and Raman signals are split by a dichroic beam splitter and detected by single-photon counting avalanche photodiodes after passing band-pass filters centered at 950 and 700 nm, respectively. A near-field image is established by raster scanning the sample and continuously recording the Raman and PL signal. Raman and PL spectra are recorded by a combination of a spectrograph and a thermoelectrically cooled charged coupled device. Sharp gold tips with a radius of 10−15 nm are produced by electrochemical etching in HCl. To establish a strong field enhancement at the tip in our on-axis illumination scheme, we use a radially polarized laser beam.[15,16]

* Corresponding author. E-mail: achim.hartschuh@uni-tuebingen.de.
† Institute of Physical and Theoretical Chemistry, University of Tuebingen.
‡ The Institute of Optics, University of Rochester.

10.1021/nl051775e CCC: $30.25
Published on Web 10/19/2005

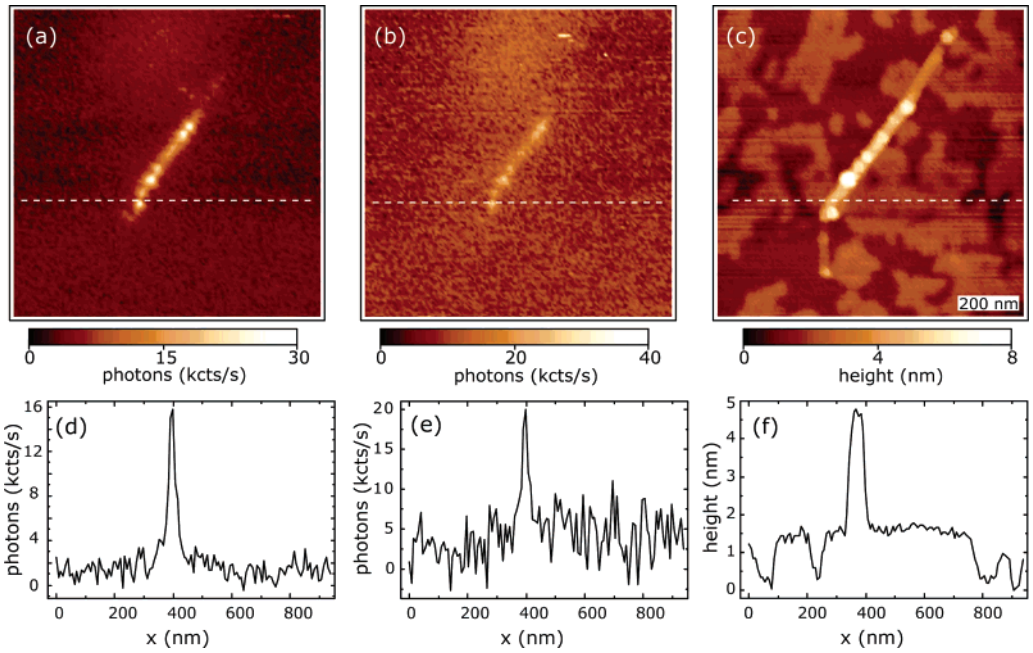

Figure 1. Near-field PL (a), Raman (b), and topography image (c) detected simultaneously for micelle-encapsulated SWNTs. (d), (e), and (f) are optical and topographic cross sections taken along the dashed lines in (a), (b), and (c), respectively.

Two different types of SWNT samples were studied. The first sample consists of micelle-encapsulated tubes[2] spin-cast on a thin layer of freshly cleaved MICA that was fixed to a microscope glass coverslip. The material for the second sample was purchased from BuckyUSA and consists of purified SWNTs with a broad diameter distribution from 0.7 to 1.8 nm, produced by arc discharge using Ni/Y catalyst particles. The material was dispersed in dichlorethene, sonicated for 1 h, and spin-cast on a microscope glass coverslip. Atomic force microscope measurements were performed to determine sample coverage.

In Figure 1a, a near-field PL image of micelle-encapsulated SWNTs on mica is shown together with the simultaneously acquired Raman (Figure 1b) and topography image (Figure 1c) of the same sample area. The PL image and the Raman image were formed by detecting the light intensity that is transmitted by the band-pass filters centered at 950 and 700 nm, respectively. Emission at 950 nm is expected to result from (8,3)-nanotubes.[17] For a laser wavelength of 632.8 nm, Raman scattered light at about 700 nm results from G-band scattering.[18] All three images are closely correlated. Besides nanotubes, the topography image also reveals two-dimensional features with a step height of about 1.4 nm as would be expected for a single layer of sodium dodecyl sulfate (SDS) surfactant.[2] The topographic height measured across the nanotubes is about 3.5 nm as can be seen from Figure 1f. On the basis of the topography data, it is not possible to distinguish between a thin bundle of nanotubes or an individual nanotube that is partially covered with SDS. The width of the observed optical signals is determined from the cross section shown in Figure 1d and Figure 1e to be about 12 nm. Remarkably, the PL is found to be extended along the nanotube, for the present example in Figure 1a on a length scale of about 500 nm, as would be expected for unperturbed and mobile excitonic states.

Near-field PL spectra taken along the nanotube in steps of 30 nm are presented in Figure 2a. From the spectra it is clear that the observed PL emission is in fact composed of multiple emission bands with different emission energies and varying relative contributions. Due to its limited spatial resolution, standard confocal spectroscopy would only show a single broadened luminescence peak resulting from a superposition of individual bands.

Similar experiments were also performed on arc-discharge SWNTs. These nanotubes were spin-cast directly on glass and were found to luminesce even without field enhancement from the metal tip although somewhat weaker as compared to those from the micelles suspension. In addition, the width of the distribution of emission energies and the average bandwidth was increased with respect to those observed for micelle-encapsulated nanotubes.[8]

Figure 3a and Figure 3c show near-field PL images typical for arc-discharge SWNTs on glass. Extremely strong luminescence is found to occur in confined segments of 20−30 nm often separated by dark sections as seen in Figure 3c. These highly luminescent but short segments indicate the presence of localized excited states. Localization could result from chirality variations along the nanotube induced, for example, by structural defects. A change in chirality can turn a luminescent nanotube into a nonluminescent one.[11,19] This would also explain the dark segments observed in Figure 3c. Other possibilities for localized emission include the trapping of energy by lower lying excited states related to charged defects or local environmental perturbations.

Figure 3b depicts the near-field Raman image of the nanotube shown in Figure 3a. The simultaneously recorded PL and Raman images allow for a quantitative comparison of the signal enhancements achieved for the different signals. In the following, the signal enhancements, defined here as the ratio between the signal amplitudes in the presence and

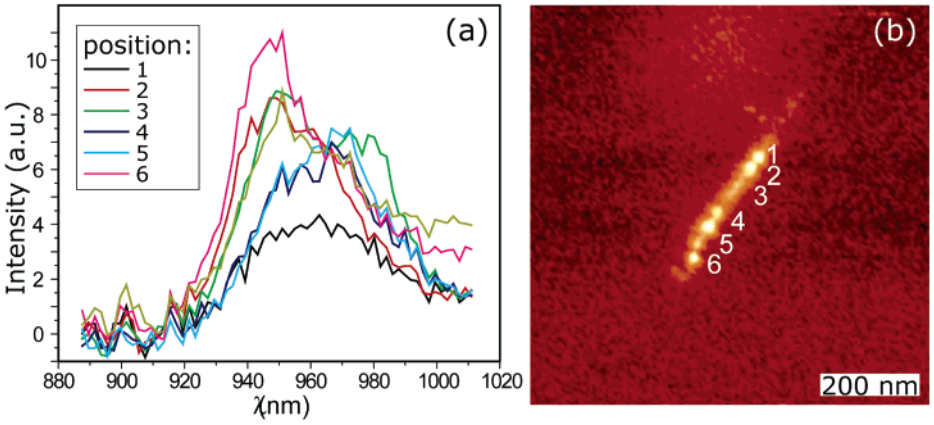

Figure 2. (a) Near-field PL spectra taken along positions 1−6 indicated in the near-field PL image of the SWNT in (b).

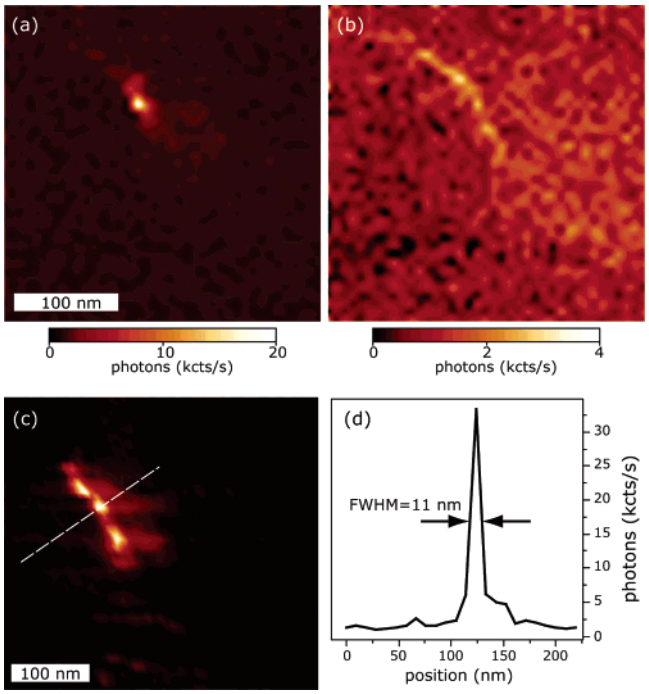

Figure 3. (a) and (c) show near-field PL images (emission intensity at 950 nm) representative for arc-discharge SWNTs on glass. (b) Simultaneously observed Raman image (G-band intensity at 700 nm) of the sample area shown in (a). (d) cross section taken along the dashed line in (c).

the absence of the tip, are discussed for the data shown in Figure 3. The tip-enhanced PL signal corresponds to 17000 photon counts/s while without tip no signal could be observed for the present tube. Using the background noise in the PL measurement of about 200 counts/s, a lower limit for the signal enhancement of $S_{PL} \approx (17000 + 200)/200 \approx 100$ can be given. For the Raman signal, a far smaller enhancement of about $S_{Raman} \approx 3$ is determined based on a near-field to far-field ratio of $S_{Raman} \approx 6000/2000$. In all observed cases, the signal enhancement for PL is significantly stronger than that for Raman scattering ranging from $S_{PL}/S_{Raman} \approx 3$ to 30.

In general, tip-enhanced near-field optical spectroscopy makes use of the strongly enhanced electric field components close to a sharp metal tip under laser illumination. The resulting enhancement for Raman scattering and PL however is expected to be different. For Raman scattering, the electromagnetic enhancement of the signal is caused by enhancement of both the incident field E_o and the scattered field. Ignoring the much weaker chemical enhancement, we can represent the overall Raman enhancement as $S_{Raman} \approx (E_{local}/E_o)^4$, where E_{local} is the local electric field. On the other hand, the PL intensity depends on the excitation rate and the quantum yield η denoting the fraction of transitions from excited state to ground state that give rise to an emitted photon. Accordingly, the PL enhancement due to the presence of the metal tip can be written as $S_{PL} \approx (E_{local}/E_o)^2 (\eta_{local}/\eta_o)$. Here, we have assumed that the system is excited far from saturation and we have ignored any vectorial field projections on the transition dipole axis. In terms of the Raman enhancement, the PL enhancement can be written as $S_{PL} \approx (S_{Raman})^{1/2}(\eta_{local}/\eta_o)$, which indicates that $S_{PL} > S_{Raman}$ is only possible if $\eta_{local}/\eta_o \gg 1$. In other words, the presence of the metal tip leads to a considerable increase of the quantum yield. Because the quantum yield cannot be larger than unity, $S_{PL} > S_{Raman}$ requires an unperturbed (intrinsic, in the absence of the tip) quantum yield that is very small, i.e., $\eta_o \ll 1$.

The quantum yield can be expressed as $\eta = \Gamma_r/(\Gamma_r + \Gamma_{nr})$, where Γ_r is the radiative decay rate and Γ_{nr} denotes the nonradiative decay rate. Both rates are affected by the presence of the tip: Γ_r is modified by the enhanced fields at the molecule location (Purcell effect) and Γ_{nr} is increased by nonradiative decay channels created by light absorption inside the metal tip.[20,21] Consequently, a strong enhancement of the PL rate requires a considerable increase of the radiative rate Γ_r due to the presence of the metal tip. In the following, we discuss our experimental findings on the signal enhancement of SWNTs and compare it with the results obtained for fluorescent molecules and semiconductor quantum dots in the literature.

The PL quantum yield of SWNTs is very low ($\eta_o \approx 10^{-3}$–10^{-4})[1,2] and can thus be increased essentially by an enhancement of the radiative rate Γ_r. Such an increase is not possible for systems with a quantum yield close to 1 such as fluorescent dyes or quantum dots. For these systems, efficient energy transfer to the metal tip was found to predominantly reduce the signal strength.[12,13] In the case of nanotubes, on

the other hand, the excited state lifetime without tip is extremely short, in the range of a few picoseconds[1,7] as compared to lifetimes in the nanosecond regime for molecules and quantum dots. Thus, a competing energy transfer to the metal tip will have a much weaker impact in the case of SWNTs.

For fluorescent molecules and quantum dots the excitation rate and the quantum yield depend on the tip−dipole distance and the mutual orientation of tip and transition dipole moment.[12,13,20] On the other hand, SWNTs are characterized by extended electronic states (delocalized excitons) for which the situation is more complex. The contact potential of the tip can influence the energetic position of electronic states. Alternatively, the tip can induce a localization of excitons accompanied with an increase in the PL quantum yield. A high susceptibility of the electron binding energies in SWNTs to changes in the dielectric environment is expected from theory.[22]

In summary, we presented the first near-field photoluminescence images of single-walled carbon nanotubes with a spatial resolution of less than 15 nm. For different tube samples, strong and highly localized PL from short tube segments has been observed. On the basis of simultaneously recorded Raman scattering images, the signal enhancements for PL and Raman scattering have been discussed quantitatively. We expect that simultaneous Raman scattering and PL spectra measured on individual SWNTs will reveal a possible correlation between structural defects and the emission properties of SWNTs.

Acknowledgment. The authors thank G. Schulte for valuable experimental support. This work was supported by the DFG through Grant ME1600/5-1 and the U.S. Department of Energy through Grant DE-FG02-01ER15204.

References

(1) Wang, F.; Dukovic, G.; Brus, L. E.; Heinz, T. F. *Phys. Rev. Lett.* **2004**, *92*, 177401−177404.
(2) O'Connell, M. J.; Bachilo, S. M.; Huffman, C. B.; Moore, V. C.; Strano, M. S.; Haroz, E. H.; Rialon, K. K.; Boul, P. J.; Noon, W. H.; Kittrell, C.; Ma, J.; Hauge, R. H.; Weisman, R. B.; Smalley, R. E. *Science* **2002**, *297*, 593−596.
(3) Ma, Y. Z.; Stenger, J.; Zimmermann, J.; Bachilo, S. M.; Smalley, R. E.; Weisman R. B.; Fleming, G. R. *J. Chem. Phys.* **2004**, *120*, 3368−3373.
(4) Zhao, H.; Mazumdar, S. *Phys. Rev. Lett.* **2004**, *93*, 157402−157405.
(5) Reich, S.; Thomsen, C.; Robertson, J. *Phys. Rev. Lett.* **2005,** *95*, 077402−077405.
(6) Perebeinos, V.; Tersoff, J.; Avouris, Ph. cond-mat/0506775.
(7) Hagen, A.; Steiner, M.; Raschke, M. B.; Lienau, C.; Hertel, T.; Qian, H.; Meixner, A. J.; Hartschuh, A. *Phys. Rev. Lett*, in press.
(8) Hartschuh, A.; Pedrosa, H. N.; Novotny, L.; Krauss, T. D. *Science* **2003**, *301*, 1293−1295.
(9) Htoon, H.; O'Connell, M. J.; Cox, P. J.; Doorn, S. K.; Klimov, V. I. *Phys. Rev. Lett.* **2004**, *93*, 027401−024704.
(10) Hartschuh, A.; Sánchez, E. J.; Xie, X. S.; Novotny, L. *Phys. Rev. Lett.* **2003**, *90*, 095503−095506.
(11) Anderson, N.; Hartschuh, A.; Cronin, S.; Novotny, L. *J. Am. Chem. Soc.* **2005**, *127*, 2533−2537.
(12) Frey, H. G.; Witt, S.; Felderer, K.; Guckenberger, R. *Phys. Rev. Lett.* **2004**, *93*, 200801−200804.
(13) Farahani, J. N.; Pohl, D. W.; Eisler, H.-J.; B. Hecht, B. *Phys. Rev. Lett.* **2005**, *95*, 017402−017405.
(14) Karrai, K., Grober, R. D. *Appl. Phys. Lett.* **1995**, *66*, 1842−1844.
(15) Novotny, L.; Bian, R. X.; Xie, X. S. *Phys. Rev. Lett.* **1997**, *79*, 645−648.
(16) Dorn, R.; Quabis, S.; Leuchs, G. *Phys. Rev. Lett.* **2003**, *91*, 233901−233904.
(17) Bachilo, S. M.; Strano, M. S.; Kittrell, C.; Hauge, R. H.; Smalley, R. E.; Weisman, R. B. *Science* **2002**, *298*, 2361−2366.
(18) Jorio, A.; Souza Filho, A. G.; Dresselhaus, G.; Dresselhaus, M. S.; Swan, A. K.; Ünlü, M. S.; Goldberg, B. B.; Pimenta, M. A.; Hafner, J. H.; Lieber, C. M.; Saito, R. *Phys. Rev. B* **2002**, *65*, 155412−155420.
(19) Doorn, S. K.; O'Connell, Zheng, L.; Zhu, Y. T.; Huang, S.; Liu, J. *Phys. Rev. Lett.* **2005**, *94*, 016802−016805.
(20) Thomas, M.; Carminati, R.; Arias-Gonzalez, J. R.; Greffet, J.-J. *Appl. Phys. Lett.* **2004**, *85*, 3863−3865.
(21) Chance, R. R.; Prock, A.; Silbey, R. *J. Chem. Phys.* **1974**, *60*, 2744−2748.
(22) Perebeinos, V.; Tersoff, J.; Avouris, Ph. *Phys. Rev. Lett.* **2004**, 92, 257402−257405.

NL051775E